



Design, synthesis and SAR studies of tripeptide analogs with the scaffold 3-phenylpropane-1,2-diamine as aminopeptidase N/CD13 inhibitors

Luqing Shang^a, Hao Fang^a, Huawei Zhu^a, Xuejian Wang^a, Qiang Wang^a, Jiajia Mu^a, Binghe Wang^b, Shiroh Kishioka^c, Wenfang Xu^{a,*}

^a Department of Medicinal Chemistry, School of Pharmacy, Shandong University, 44 West Culture Road, 250012 Ji'nan, Shandong, PR China

^b Department of Chemistry, Georgia State University, Atlanta, 30303, USA

^c Department of Pharmacology, Wakayama Medical University, Wakayama city, Wakayama 641-8509, Japan

ARTICLE INFO

Article history:

Received 12 January 2009

Revised 15 February 2009

Accepted 18 February 2009

Available online 24 February 2009

Keywords:

Aminopeptidase N inhibitor

3-Phenylpropane-1,2-diamine

Tripeptide analogs

Synthesis

ABSTRACT

Aminopeptidase N (APN), belonged to metalloproteinase, is an essential peptidase involved in the process of tumor invasion and metastasis. A series of tripeptide analogs with the scaffold 3-phenylpropane-1,2-diamine were designed, synthesized and evaluated for their ability to inhibit APN. Preliminary activity evaluation showed that most of target compounds possessed potent inhibitory activities against APN. With in this series, compound **A6** and **B6** exhibited good potency with the IC₅₀ values of $8.8 \pm 1.3 \mu\text{M}$ and $8.6 \pm 1.1 \mu\text{M}$, respectively.

© 2009 Elsevier Ltd. All rights reserved.

1. Introduction

As a Zn²⁺-dependent exopeptidase, aminopeptidase N (APN) is expressed by myeloid, monocytes, epithelial cells of the intestine and kidney, fibroblasts, endothelial cells and is over-expressed on tumor cells.¹ The enzyme is identical to human lymphocyte surface cluster differentiation antigen, CD13.² Being responsible for the cleavage the N-amino group from polypeptide chains, APN plays a key role in physiological processing and degradation of peptides and proteins, and alterations in their activity have been associated with various pathological disorders.^{3–6}

Since 1976, several excellent reviews on natural and synthetic small molecule inhibitors of APN have been published.^{7–9} Among these inhibitors, the best well known is bestatin, which was isolated by Umezawa et al. in a search for low molecular weight inhibitors for hydrolytic enzymes on the surfaces of cells.¹⁰

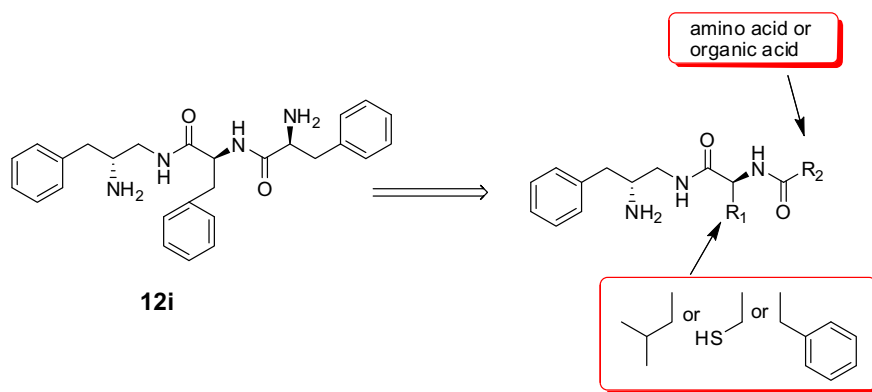
The 3D-structures of APN have been investigated by the X-ray crystallographic studies on the co-crystal of the enzyme and various inhibitors.^{11–13} Our group had reported some novel APN inhibitors, such as 3-galloylamido-*N*-substituted 2,6-piperidinedione-*N*-acetamide peptidomimetics,¹⁴ *L*-lysine derivatives,¹⁵ *L*-glutamine derivatives¹⁶ and AHPA (β -Amino- α -hydroxyl-phenylbutanoic acid) derivatives.¹⁷ Kiyoshi et al. had reported the binding site and cata-

lytic domain of APN based on the co-crystal complex of APN and bestatin.¹² The binding site of the APN with bestatin can be divided to three parts, part A is a hydrophobic pocket (S₁) which interacts with phenyl group of bestatin; part B is the zinc binding group (ZBG) and part C is another hydrophobic pocket in other side. Additionally, part C can be divided into pocket S'₁ and pocket S'₂ in details.^{7,15,18}

During our previous work, we have reported 3-phenylpropane-1,2-diamine derivatives possessed APN inhibitory activities.¹⁹ Most importantly, the tripeptide analog compound **12i** *L*-phenylalanyl-*N*-[(2*R*)-2-amino-3-phenylpropyl]-*L*-phenylalaninamide exhibited good enzymatic inhibition against APN (IC₅₀: 15.5 μM). The hydrophobic pocket S₁, S'₁ and S'₂ were occupied by three aryl ring, respectively. Additionally, the carbonyl group of compound **12i** could bind to the zinc ion in the active pocket with distance of 2.04 Å. In this work, we wanted to use compound **12i** as lead compound to design and synthesize tripeptide analogs with 3-phenylpropane-1,2-diamine as scaffold. In order to find better APN inhibitors, we modified the structure as the following: (i) R₁ amino acid we first introduced was *L*-phenylalanine, the same as the compound **12i**. (ii) R₁ amino acid we then introduced was *L*-cysteine because we presumed the thiol group may increase the activity of target compounds according to the literature.²¹ (iii) R₁ amino acid we last introduced was *L*-leucine in order to investigate whether the alkyl group increase the activity of the target compounds or not. (iv) R₂ we introduced were various amino acids or organic acids.

* Corresponding author. Tel./fax: +86 531 88382264.

E-mail address: wfxu@yahoo.cn (W. Xu).



2. Chemistry

The target compounds were synthesized efficiently following the procedures as shown in Scheme 1. The starting material compound **1** (2*R*)-2-[(*tert*-butoxycarbonyl) amino]-3-phenyl-propanol was prepared from *D*-phenylalanine according to the literature.²⁰

The hydroxyl group of compound **1** was converted to mesyl group by methanesulfonyl chloride and then reacted with sodium azide to generate azide **3**. The compound **3** underwent disoxidation using magnesium in methanol to provide the key intermediate **4**.

The compound **7** was obtained by the condensation of the methyl ester **5** and the compound **6**. Hydrolysis of the compound **7** with NaOH/H₂O yielded the dipeptidomimetics **8**.

The compound **8** were activated with isobutyl chloroformate and *N*-methylmorpholine and then coupled with compound **4** to yield **9**. The Boc-protecting group can be easily removed by 3 N HCl in ethyl acetate to give hydrochloride salts **10**.

3. Result and discussion

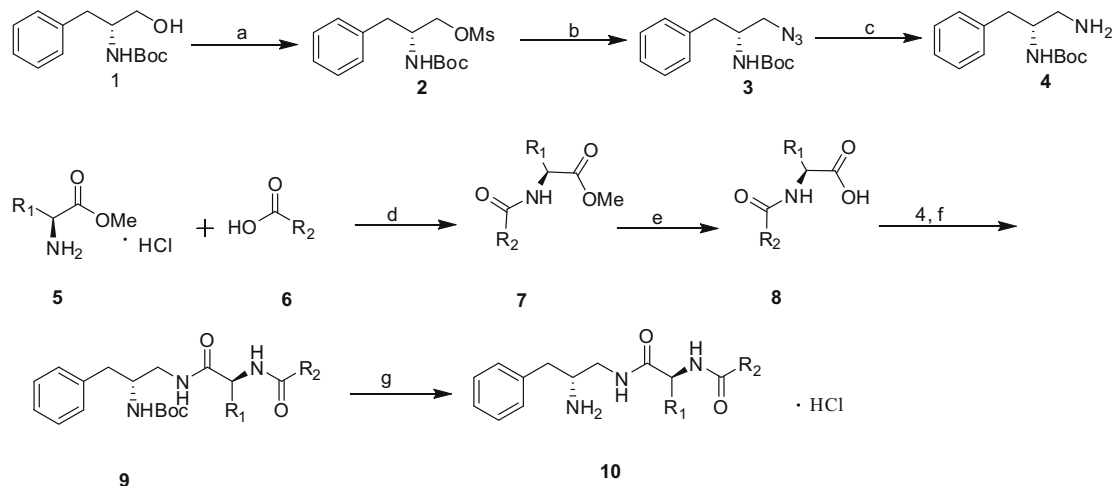
The preliminary pharmacological studies of all the target compounds have been investigated on enzymatic inhibition of APN and the result listed in Table 1. Compared with those compounds in the previous work,¹⁹ preliminary result showed that most of target compounds displayed better APN inhibitory activities than before.

As shown in the results, compound **B1**, **B3**, **B6**, **A6** exhibited better activities than the lead compound **12i** and compound **B5** and **B8**

also showed similar activities to compound **12i**. In addition, the effects of **B1**, **B3**, **B4**, **B5**, **B6**, **A4** and **A6** on the HL-60 cell proliferation compared with bestatin were shown in Figure 1. Cell viability was assessed by MTT method. Compound **B6** and **A6** exhibited the inhibitory effect of cell proliferation with IC₅₀ values of 0.29 ± 0.06 mM and 0.27 ± 0.08 mM, respectively, which showed better potency than that of bestatin with IC₅₀ value of 0.92 ± 0.12 mM (Table 2).

Comparing the IC₅₀'s of compounds **B1–B11** contained thiol group with those of compounds **A1–A13** contained phenyl group and compounds **C1–C7** contained isobutane group, the inhibitory activities of **B** series (R₁: –CH₂SH) were generally better than **A** series (R₁: –CH₂Phe) and **C** series (R₁: –CH₂CH(CH₃)₂). It may be caused by the thiol group in the **B** series. Fournié-Zaluski et al. had reported β-amino-thiols inhibitors containing a thiol group as ZBG showed well APN inhibitory potency.²¹ When the R₂ group was fixed, the activities of compounds in **A** series and **C** series (e.g., **A7** and **C5**, **A9** and **C1**) were similar. Among all of the target compounds, when the R₁ group was fixed, the R₂ group was altered from amino acid to organic acid. The compounds bearing amino acids were found to be more potent than the compounds bearing organic acids. This result might be owing to the amino group of the amino acid which could interact with the carbonyl group of the residue of amino acid in the active site of APN.

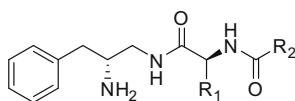
In order to investigate the interaction of our target compounds with APN, the representative compound **B6** was constructed with Sybyl/Sketch module and optimized using Powell's method with



Scheme 1. Reagents and conditions: (a) MsCl/THF, 0 °C; (b) NaN₃/DMF; (c) Mg/MeOH; (d) isobutyl chloroformate, *N*-methylmorpholine, THF, –15 °C; (e) NaOH, MeOH; acetic acid, H₂O; (f) isobutyl chloroformate, *N*-methylmorpholine, THF, –15 °C; (g) HCl/EtOAc.

Table 1

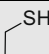
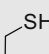
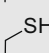
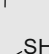
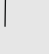
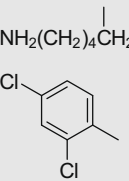
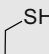
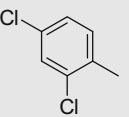
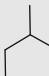
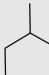
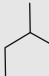
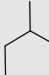
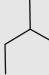
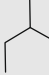
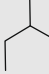
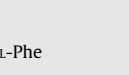
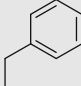
The structures and in vitro activities of target compounds against APN



No.	R ₁	R ₂	IC ₅₀ ^a (μM)	Actual pIC ₅₀	Predicted pIC ₅₀	Residual
A1		L-Val	58.5 ± 1.8	4.23	4.16	0.07
A2			277.2 ± 2.6	3.56	3.40	0.16
A3			1390.73 ± 4.4	2.86	3.01	-0.15
A4		L-Lys	89.5 ± 2.1	4.05	4.38	-0.33
A5 ^b		NH ₂ (CH ₂) ₄ CH ₃	1538.8 ± 3.8	2.81	3.44	-0.63
A6		L-Met	8.8 ± 1.3	5.05	4.96	0.09
A7		L-Cys	49.2 ± 2.2	4.31	4.08	0.23
A8		L-Leu	180.9 ± 3.8	3.74	4.02	-0.28
A9 ^b		L-Ile	157.9 ± 3.3	3.8	4.26	-0.46
A10		Cl(CH ₂) ₃ -	692.8 ± 4.8	3.16	3.41	-0.25
A11			2262.6 ± 5.4	2.65	2.70	-0.05
A12		PheCH ₂ CH ₂ -	366.0 ± 3.6	3.44	3.46	-0.02
A13		4-CH ₃ O-Phe-	173.6 ± 3.0	3.76	3.55	0.21
B1		L-Phe	9.8 ± 1.3	5.01	5.20	-0.19
B2		Gly	173.7 ± 2.6	3.76	3.86	-0.10
B3		L-Cys	10.3 ± 1.5	4.99	4.52	0.47
B4		L-Leu	45.0 ± 1.5	4.35	4.41	-0.06
B5 ^b		L-Met	16.5 ± 21.3	4.78	4.58	0.20

(continued on next page)

Table 1 (continued)

No.	R ₁	R ₂	IC ₅₀ ^a (μM)	Actual pIC ₅₀	Predicted pIC ₅₀	Residual
B6		L-Lys	8.6 ± 1.1	5.07	4.77	0.30
B7		L-Orn	33.2 ± 2.0	4.48	4.67	-0.19
B8		L-Ile	14.8 ± 1.8	4.83	4.64	0.19
B9		L-Val	58.8 ± 2.1	4.23	4.54	-0.31
B10^b		NH ₂ (CH ₂) ₄ CH ₂ 	202.4 ± 2.9	3.69	3.79	-0.10
B11			1048.89 ± 4.2	2.98	3.04	-0.06
C1		L-Ile	147.6 ± 2.8	3.83	3.70	0.13
C2		L-Leu	142.1 ± 2.3	3.85	3.47	0.38
C3		L-Ala	521.5 ± 3.8	3.28	3.21	0.07
C4^b		Gly	3244.4 ± 4.8	2.49	2.90	-0.41
C5^b		L-Cys	30.4 ± 1.9	4.52	4.39	0.13
C6		L-Tyr	106.9 ± 3.2	3.97	4.19	-0.22
C7		NH ₂ (CH ₂) ₄ CH ₂ 	1457.4 ± 4.3	2.84	2.88	-0.04
12i		L-Phe	15.5 ± 1.2	4.81	4.80	-0.01
	Bestatin		3.1 ± 0.6			

^a Each value represents the mean of three experiments, standard deviation is given.^b Molecules in test set.

the Tripos force field with convergence criterion set at 0.05 kcal/(Å mol), and assigned with Gasteiger–Hückel method. The docking study performed using Sybyl/FlexX module, the residues in a radius of 7.0 Å around bestatin in the co-crystal structure (PDB code: 2DQM) were selected as the active site. Other docking parameters implied in the program were kept default. The binding studies showed the carbonyl group of compound **B6** coordinated to the zinc ion in the active site. In addition, the phenyl group inserted to S₁ pocket, the thiol group orientated to S'₁ pocket and the lysine side chain plunged into pocket S'₂ (Fig. 2A). The tripeptide analog **B6** formed a hydrogen bond with the carbonyl group of Glu²⁶⁴, in a way similar to that of APN peptide substrate and APN (in which Glu²⁶⁴ could recognize the amino acid of substrate¹²). In addition, two amino groups of the lysine side chain of compound **B6** could form hydrogen bond with the oxygen atom of Tyr²⁷⁵ and Tyr³⁸¹, respectively. Tyr³⁸¹ had been reported to be benefit to stabilize of the reaction intermediate with the zinc ion¹² (Fig. 2B).

4. SAR studies

4.1. Dataset and molecular modeling

In order to achieve a quantitative understanding between the APN inhibitory activity and molecular structure of the synthesized compounds, a three dimensional quantitative structure activity relationship (3D-QSAR) study was performed using Comparative Molecular Field Analysis (CoMFA) method implemented in SYBYL 7.0. The CoMFA method is a widely accepted 3D-QSAR strategy, and has been applied in the previous study of our group.

Here the leading compound **12i** was chosen as the template compound and its docking conformation reported in our earlier publication¹⁸ was used as the alignment template. The rest 31 molecules were sketched based on the template conformation and aligned with the common structure (Fig. 3). Then the whole alignment set was assigned with Gasteiger–Hückel partial charge. The

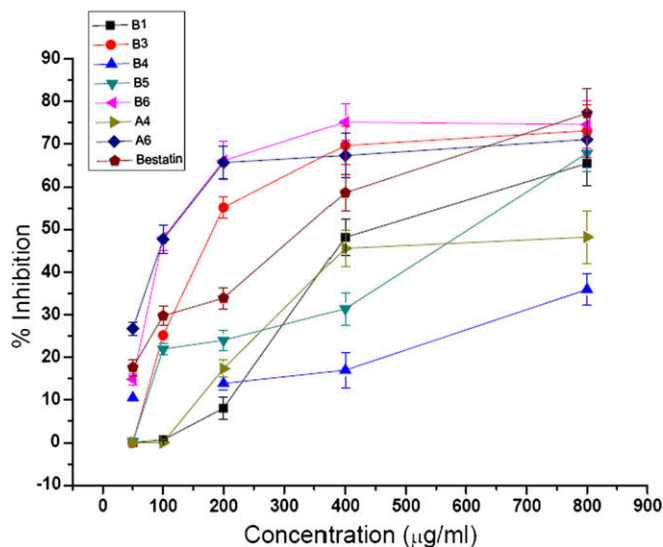


Figure 1. Effects of bestatin and compound **B1**, **B3**, **B4**, **B5**, **B6**, **A4**, **A6** on the HL-60 cell line proliferation. Each column represents the mean with S.E. of five independent experiments.

Table 2

The results of target compounds on HL-60 cell line proliferation

Compound	IC ₅₀ (mM)	Compound	IC ₅₀ (mM)
Bestatin	0.92 ± 0.12	B5	1.18 ± 0.15
B1	1.06 ± 0.22	B6	0.29 ± 0.06
B3	0.54 ± 0.12	A4	1.49 ± 0.21
B4	2.66 ± 0.25	A6	0.27 ± 0.08

biological data obtained as IC₅₀ (μM) were converted into pIC₅₀ (−LogIC₅₀) values and used as dependent variables in the 3D-QSAR analyses (Table 1). Six molecules were randomly picked out and assigned as the test set. The remaining molecules as the training set were used to generate the CoMFA model (Table 1).

CoMFA steric and electrostatic fields were generated using Leonard-Jones and Coulombic potential, respectively. A sp³ carbon atom with +1.00 charge was used as probe atom. The steric and electrostatic CoMFA fields were calculated at each lattice intersection of a regularly spaced grid of 2.0 Å in all three dimensions within defined region. The Leave-One-Out (LOO) cross-validation process, with SAMPLS method, was firstly used to seek the optimum number of components (ONC), and then the CoMFA model was computed with non-cross-validation PLS at the obtained ONC.

4.2. Results and discussion

From the statistics of PLS analyses (Table 3), cross-validated coefficient q^2 of 0.583 and the R^2 (Test set) of 0.658 showed that our CoMFA model has good predictive ability. Table 1 showed a comparison of the experimentally determined pIC₅₀ and calculated pIC₅₀ values using the CoMFA model developed, and Figure 5 showed the schematic correlation of these data. Finally, the contour maps of CoMFA model were showed in Figure 4.

Figure 4A presented the steric contour map of the CoMFA model. It suggested that the influence of steric field on APN inhibitory activity is mainly located in the R₁ and R₂ positions. The green region located near the R₂ position indicated that the bulky group here would increase the APN inhibitory activity. For example, compound **B4** and **C2** exhibited lower IC₅₀ values than these of compound **B2** and **C4**, mainly for their bulky groups in the R₂ position. The green and yellow regions around the R₁ position suggested there should be bulky group in R₁ position, but the substituent should not be too big. The CoMFA electrostatic contour map represent in Figure 4B, which include a blue region and a red region. The blue region indicates that the presence of positively charged groups would increase the activity. So compounds did not have a free amino group at R₂ position (e.g., **A5**) usually less potent than those have (e.g., **A1**). The red region adjacent to the R₂ group indicated negatively charged groups at this position would increase activity (e.g., **B3**).

5. Conclusions

In summary, we have described the synthesis and properties of a series of tripeptide analogs with the scaffold 3-phenylpropane-1,2-diamine. Most of compounds possess potent APN inhibitory activity and the most potent compounds, **A6** and **B6**, exhibited good enzymatic inhibition against APN. A consistent binding mode established was critical to predictive structure based drug design and the properly substituted 3-phenylpropane-1,2-diamine provide an attractive structural template for developing potent APN inhibitors.

6. Experimental

6.1. Chemistry: general procedures

Unless specified otherwise, all starting material, reagents and solvents were commercially available. All reactions except those in aqueous media were carried out by standard techniques for

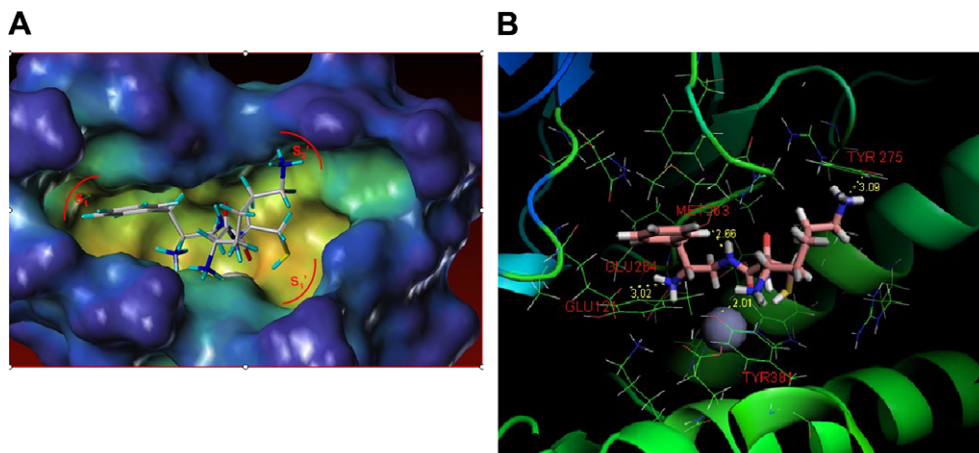


Figure 2. (A) The FlexX docking result of **B6** with APN; (B) The FlexX docking result of **B6** showed by PyMOL.

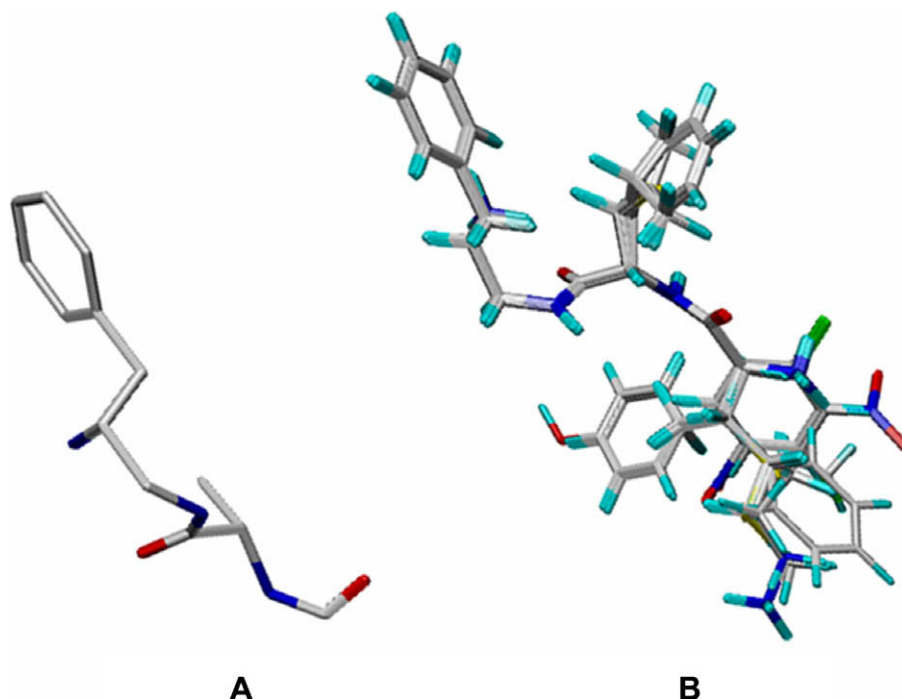


Figure 3. (A) The common structure used in molecular alignment. (B) Structural alignments of the compounds in the training set and test set for constructing 3D-QSAR CoMFA model.

Table 3
Statistics of CoMFA PLS analyses

Statistical parameters	Values
q^2	0.583
ONC	5
R^2 (Training set)	0.915
SEE	0.241
F	43.018
R^2 (Test set)	0.658
Fraction of field contributions	
Steric	71.2%
Electrostatic	28.8%

the exclusion of moisture. All reactions were monitored by thin-layer chromatography on 0.25 mm silica gel plates (60GF-254) and visualized with UV light, or iodine vapor. Proton NMR spectra were determined on a Bruker DRX spectrometer operating at 300 MHz for ^1H , δ in parts per million and J in hertz, using TMS as an internal standard. ESI-MS were determined on an API 4000 spectrometer. Measurements were made in D_2O or CD_3OD solutions. Melting points were determined on an electrothermal melting point apparatus and were uncorrected. Anhydrous reactions were carried out in over-dried glassware under a nitrogen atmosphere.

6.1.1. (2*R*)-2-[(*tert*-Butoxycarbonyl)amino]-3-phenylpropyl methanesulfonate (**2**)

Compound **1** (5 g, 20 mmol) was dissolved in anhydrous THF (20 mL) and Et_3N (3.03 g, 30 mmol) was added to the solution. A solution of methanesulfonyl chloride (3.4 g, 30 mmol) in anhydrous THF (10 mL) was added dropwise to the mixture. The reaction mixture was stirred for 4 h. The mixture was poured to the cold water and white solid was precipitated to give crude product (*R*)-2-[(*tert*-butoxycarbonyl)-3-phenylpropyl methanesulfonate (5.52 g, yield 84%), which was of suitable purity to use directly in next reaction.

6.1.2. (2*R*)-2-[(*tert*-Butoxycarbonyl)amino]-3-phenylpropylamine (**4**)

A mixture of sulfonate **2** (10 g, 30 mmol) and NaN_3 (3.95 g, 60 mmol) in anhydrous DMF (80 mL) was stirred at 60 °C for 10 h. The mixture was poured to the cold water and extracted with ethyl acetate. The organic layer was washed with water and brine, dried over Na_2SO_4 and concentrated in vacuum. The residue was purified by flash column chromatography to give on silica gel (petroleum/EtOAc 10/1) to afford compound **3** (2*R*)-*tert*-butyl (2-azido-methyl-1-benzylethyl) carbamate.

The azide **3** (4 g, 0.015 mol) was hydrogenated on Mg (1.08 g, 0.045 mol) in MeOH at ordinary pressure and 0 °C for 1 h. MeOH was removed under reduced pressure and the residue was diluted with water. The aqueous solution was extracted efficiently with ether and the ether layer was washed with brine, dried over Na_2SO_4 and concentrated in vacuum to give product **4** (2*R*)-2-[(*tert*-butoxycarbonyl)amino]-3-phenyl-propylamine. ESI-MS m/z : 251.1 ($\text{M}+\text{H}^+$); ^1H NMR (MeOD) δ 1.41(s, 9H), 2.59–2.65 ($J_1 = 6$, $J_2 = 12$, dd, 1H), 2.71–2.81 (m, 3H), 3.79 (m, 1H), 7.18–7.32 (m, 5H).

6.1.3. *N*-(*tert*-Butoxycarbonyl)-L-valyl-L-phenylalanine (**8-A1**)

To a stirred solution of *N*-*tert*-butoxycarbonyl-L-valine (1.39 g, 4.40 mmol) and *N*-methylmorpholine (0.53 mL, 4.80 mmol) in THF (15 mL) was added isobutyl chloroformate (0.62 mL, 4.80 mmol) at –15 °C. The mixture was stirred for 30 min at the same temperature. L-Methyl phenylalaninate (0.95 g, 4.40 mmol) was added to the mixture. The stirring was continued for 1 h at –15 °C and then remove the cooling bath. The reaction was continued for 4 h and the mixture was concentrated with a rotary evaporator. The residue was dissolved in EtOAc and washed with 5% NaHCO_3 , 10% citric acid, and brine in turn. The EtOAc solution was dried over Na_2SO_4 and concentrated with a rotary evaporator to afford crude product **7-A1**.

Compound **7-A1** (1.5 g, 4.12 mmol) was dissolved in MeOH (40 mL), and 10 mL of 1 mol/L NaOH was added over 5 min with good stirring. The reaction mixture was stirred for 5 h at room temperature. The pH of the resulting solution was adjusted to 7–8 with

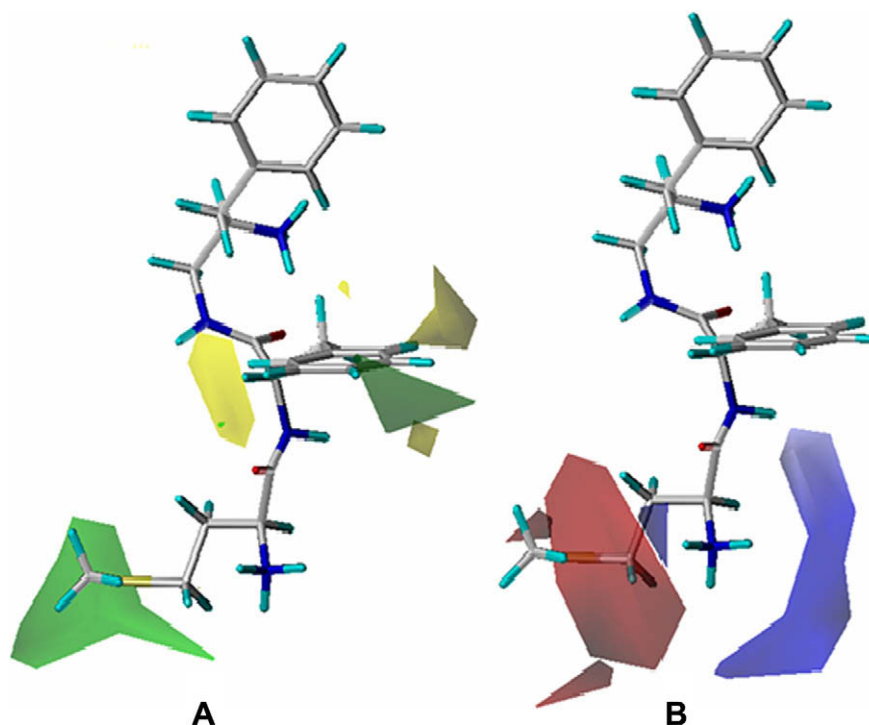


Figure 4. Contour maps of CoMFA model, compound **A6** was taken as the reference molecule. All the map regions represent in transparent view mode. (A) Steric contour maps of CoMFA model, green indicates regions where bulky groups increase activity, yellow indicates regions where bulky groups decrease activity. (B) Electrostatic contour maps of CoMFA model, blue indicates regions where more positively charged groups increase activity, red indicates regions where more negatively charged groups increase activity.

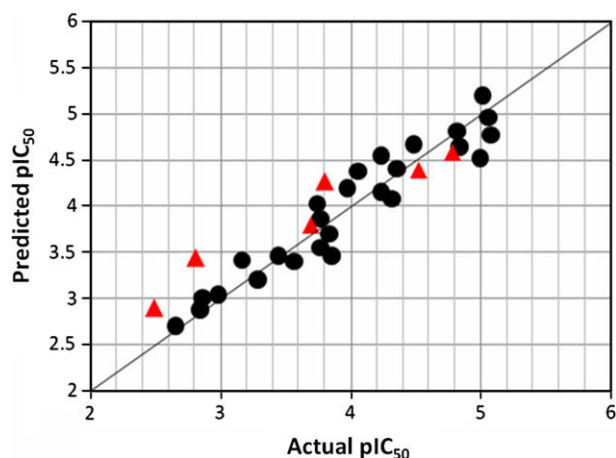


Figure 5. Scatter plots of the CoMFA predicted and experimental values of APN inhibitory activity. ● represents the molecule used in training set; ▲ represents the molecule used in test set.

80% acetic acid/water and compound **8-A1** precipitated as a white solid, which was collected by filtration and dried and was of suitable purity to use directly in next reaction.

6.1.4. *N*-(*tert*-Butoxycarbonyl)-*L*-valyl-*N*-[(2*R*)-2-[(*tert*-butoxycarbonyl)amino]-3-phenylpropyl]-*L*-phenylalaninamide (**9-A1**)

To a stirred solution of compound **8-A1** (1.3 g, 3.57 mmol) and *N*-methylmorpholine (0.48 mL, 4.28 mmol) in THF (15 mL) was added isobutyl chloroformate (0.57 mL, 4.28 mmol) at -15°C . The mixture was stirred for 30 min at the same temperature. A solution of compound **4** (2*R*)-2-[(*tert*-butoxycarbonyl)amino]-3-phenyl-propylamine (0.89 g, 3.57 mmol) in THF

(20 mL) was added dropwise to the reaction mixture. The stirring was continued for 1 h at -15°C and then remove the cooling bath. The reaction was continued for 4 h and the mixture was filtrated. After filtration, the filtrate was concentrated with a rotary evaporator. The residue was dissolved in EtOAc and washed with 5% NaHCO_3 , 10% citric acid, and brine in turn. The EtOAc solution was dried over Na_2SO_4 and concentrated with a rotary evaporator to afford crude product. The crude product was recrystallized by EtOAc to afford pure title compound **9-A1**. Yield: 66%, mp = $110\text{--}112^{\circ}\text{C}$. ESI-MS m/z : 597.6 ($\text{M}+\text{H}^+$); ^1H NMR (MeOD) δ 0.91–0.94 (J = 8.7, d, 6H), 1.27 (s, 9H), 1.38 (s, 9H), 2.10–2.16 (m, 1H), 2.80–2.82 (J = 6.3, d, 2H), 3.01–3.07 (m, 2H), 3.12–3.19 (m, 1H), 3.51–3.55 (m, 2H), 3.69–3.71 (J = 5.4, d, 1H), 4.47–4.51 (J = 14.4, t, 1H), 7.15–7.36 (m, 10H).

6.1.5. *L*-Valyl-*N*-[(2*R*)-2-amino-3-phenylpropyl]-*L*-phenylalaninamide hydrochloride (**A1**)

Compound **9-A1** (1 g, 1.67 mmol) was dissolved in 20 mL HCl-EtOAc (3 mol/L). After 30 min, the solvent was filtrated and the precipitate was washed with EtOAc to get 0.49 g of compound **A1** as a white solid. Yield: 73%, mp = $167\text{--}169^{\circ}\text{C}$. ESI-MS m/z : 397.6 ($\text{M}+\text{H}^+$); ^1H NMR (MeOD) δ 1.04–1.10 (m, 6H), 2.17–2.25 (m, 1H), 2.84–2.86 (J = 6.3, d, 2H), 3.06–3.12 (m, 2H), 3.15–3.23 (m, 1H), 3.50–3.55 (m, 2H), 3.72–3.74 (J = 5.7, d, 1H), 4.52–4.57 (J = 15.3, t, 1H), 7.18–7.40 (m, 10H).

6.1.6. *N*¹-[(2*R*)-2-Amino-3-phenylpropyl]-*N*-(3,5-dinitrobenzoyl)-*L*-phenylalaninamide hydrochloride (**A2**)

Yield: 75%, mp = $126\text{--}127.5^{\circ}\text{C}$. ESI-MS m/z : 492.5 ($\text{M}+\text{H}^+$); ^1H NMR (MeOD) δ 2.83–2.91 (m, 2H), 3.15–3.19 (m, 1H), 3.22–3.29 (m, 2H), 3.56–3.62 (m, 2H), 4.70–4.75 (J = 15.6, t, 1H), 7.22–7.24 (m, 2H), 7.25–7.28 (m, 2H), 7.30–7.33 (m, 3H), 7.36–7.41 (m, 3H), 9.02–9.03 (J = 2.1, d, 2H), 9.14–9.16 (J = 4.2, t, 1H).

6.1.7. *N*¹-[(2*R*)-2-Amino-3-phenylpropyl]-*N*-(4-nitrobenzoyl)-*L*-phenylalaninamide hydrochloride (A3)

Yield: 63%, mp = 228–230 °C. ESI-MS *m/z*: 447.6 (M+H)⁺; ¹H NMR (MeOD) δ 2.85–2.90 (m, 2H), 3.09–3.16 (m, 2H), 3.18–3.22 (m, 1H), 3.53–3.57 (m, 2H), 4.63–4.69 (*J* = 16.5, t, 1H), 7.22–7.27 (m, 3H), 7.28–7.30 (m, 2H), 7.30–7.32 (m, 2H), 7.34–7.40 (m, 3H), 7.99–8.02 (*J* = 8.7, d, 2H), 8.31–8.34 (*J* = 9, d, 2H).

6.1.8. *L*-Lysyl-*N*¹-[(2*R*)-2-amino-3-phenylpropyl]-*L*-phenylalaninamide hydrochloride (A4)

Yield: 72%, mp = 99–101 °C. ESI-MS *m/z*: 426.6 (M+H)⁺; ¹H NMR (MeOD) δ 1.49–1.55 (m, 2H), 1.68–1.76 (m, 2H), 1.89–1.93 (m, 2H), 2.87–2.89 (m, 2H), 2.95–3.00 (m, 2H), 3.10–3.15 (*J* = 15.3, t, 2H), 3.17–3.23 (m, 1H), 3.52–3.54 (m, 2H), 3.94–3.97 (m, 1H), 4.50–4.55 (*J* = 15.6, t, 1H), 7.22–7.41 (m, 10H).

6.1.9. *N*¹-[(2*R*)-2-Amino-3-phenylpropyl]-*N*-(6-amino-hexanoyl)-*L*-phenylalaninamide hydrochloride (A5)

Yield: 65%, mp = 244–246 °C. ESI-MS *m/z*: 411.5 (M+H)⁺; ¹H NMR (MeOD) δ 1.01–1.07 (m, 2H), 1.45–1.52 (m, 2H), 1.61–1.66 (m, 2H), 2.08–2.11 (*J* = 7.5, t, 2H), 2.89–2.96 (m, 2H), 3.02–3.08 (m, 2H), 3.11–3.16 (*J* = 15, t, 2H), 3.52–3.57 (m, 2H), 3.91–3.95 (m, 1H), 4.42–4.47 (*J* = 14.1, t, 1H), 7.21–7.43 (m, 10H).

6.1.10. *L*-Methionyl-*N*-[(2*R*)-2-amino-3-phenylpropyl]-*L*-phenylalaninamide hydrochloride (A6)

Yield: 70%, mp = 250–254 °C. ESI-MS *m/z*: 429.5 (M+H)⁺; ¹H NMR (MeOD) δ 2.04–2.09 (*J* = 15.3, t, 2H), 2.14 (s, 3H), 2.57–2.62 (*J* = 15.6, t, 2H), 2.88–2.91 (*J* = 6.6, d, 2H), 3.06–3.14 (m, 2H), 3.16–3.24 (m, 2H), 3.42–3.48 (m, 1H), 3.53–3.58 (m, 1H), 4.55–4.61 (*J* = 15.6, t, 1H), 7.23–7.41 (m, 10H).

6.1.11. *L*-Cysteinyl-*N*-[(2*R*)-2-amino-3-phenylpropyl]-*L*-phenylalaninamide hydrochloride (A7)

Yield: 71%, mp = 186–192 °C. ESI-MS *m/z*: 401.5 (M+H)⁺; ¹H NMR (MeOD) δ 2.93–2.95 (*J* = 6.3, d, 2H), 3.13–3.18 (m, 2H), 3.23–3.28 (m, 2H), 3.30–3.55 (m, 2H), 3.53–3.58 (m, 1H), 3.72–3.76 (*J* = 12.6, t, 1H), 4.52–4.67 (*J* = 15.3, t, 1H), 7.27–7.40 (m, 10H).

6.1.12. *L*-Leucyl-*N*¹-[(2*R*)-2-amino-3-phenylpropyl]-*L*-phenylalaninamide hydrochloride (A8)

Yield: 66%, mp = 140–144 °C. ESI-MS *m/z*: 411.6 (M+H)⁺; ¹H NMR (MeOD) δ 1.02–1.05 (m, 6H), 1.33–1.38 (m, 1H), 1.71–1.73 (m, 2H), 2.84–2.91 (m, 2H), 3.02–3.04 (*J* = 6.9, d, 2H), 3.46–3.55 (m, 2H), 3.67–3.70 (m, 1H), 3.74–3.77 (m, 1H), 3.96–4.01 (*J* = 14.4, t, 1H), 7.25–7.42 (m, 10H).

6.1.13. *L*-Isoleucyl-*N*¹-[(2*R*)-2-amino-3-phenylpropyl]-*L*-phenylalaninamide hydrochloride (A9)

Yield: 66%, mp = 228–230 °C. ESI-MS *m/z*: 411.6 (M+H)⁺; ¹H NMR (MeOD) δ 0.89–0.92 (*J* = 6.9, d, 3H), 0.96–1.00 (*J* = 13.8, t, 3H), 1.03–1.07 (m, 2H), 1.57–1.65 (m, 1H), 2.89–2.97 (m, 2H), 3.01–3.05 (m, 1H), 3.07–3.14 (*J* = 6.3, *J*₂ = 13.5, dd, 1H), 3.23–3.29 (*J*₁ = 4.8, *J*₂ = 14.1, dd, 1H), 3.40–3.48 (*J*₁ = 4.2, *J*₂ = 14.4, dd, 1H), 3.51–3.55 (m, 1H), 3.67–3.72 (m, 1H), 3.81–3.85 (*J* = 13.5, t, 1H), 7.22–7.39 (m, 10H).

6.1.14. *N*¹-[(2*R*)-2-Amino-3-phenylpropyl]-*N*-(4-chlorobutanoyl)-*L*-phenylalaninamide hydrochloride (A10)

Yield: 73%, mp = 100–102 °C. ESI-MS *m/z*: 402.4 (M+H)⁺; ¹H NMR (MeOD) δ 1.92–2.04 (m, 2H), 2.36–2.41 (*J* = 14.7, t, 2H), 2.88–2.91 (*J* = 14.4, t, 2H), 2.94–2.99 (m, 1H), 3.12–3.19 (m, 2H), 3.44–3.57 (m, 4H), 4.43–4.48 (*J* = 15.3, t, 1H), 7.19–7.41 (m, 10H).

6.1.15. *N*¹-[(2*R*)-2-Amino-3-phenylpropyl]-*N*-(2,4-dichlorobenzoyl)-*L*-phenylalaninamide hydrochloride (A11)

Yield: 68%, mp = 280–284 °C. ESI-MS *m/z*: 470.3 (M+H)⁺; ¹H NMR (MeOD) δ 2.90–2.92 (m, 2H), 3.03–3.10 (m, 1H), 3.17–3.24 (m, 2H), 3.56–3.59 (m, 2H), 4.65–4.67 (*J* = 6.9, t, 1H), 7.23–7.25 (m, 1H), 7.26–7.28 (m, 1H), 7.27–7.35 (m, 5H), 7.36–7.42 (m, 5H), 7.54 (s, 1H).

6.1.16. *N*¹-[(2*R*)-2-Amino-3-phenylpropyl]-*N*-(3-phenylpropanoyl)-*L*-phenylalaninamide hydrochloride (A12)

Yield: 72%, mp = 167–170 °C. ESI-MS *m/z*: 430.5 (M+H)⁺; ¹H NMR (MeOD) δ 2.50–2.55 (*J* = 15.6, t, 2H), 2.80–2.87 (m, 4H), 2.91–2.96 (m, 1H), 3.05–3.12 (m, 2H), 3.48–3.51 (m, 2H), 4.41–4.43 (m, 1H), 7.15–7.41 (m, 15H).

6.1.17. *N*¹-[(2*R*)-2-Amino-3-phenylpropyl]-*N*-(4-methoxybenzoyl)-*L*-phenylalaninamide hydrochloride (A13)

Yield: 67%, mp = 93–95 °C. ESI-MS *m/z*: 432.5 (M+H)⁺; ¹H NMR (MeOD) δ 2.88–2.98 (m, 2H), 3.10–3.18 (m, 2H), 3.20–3.27 (m, 2H), 3.55–3.59 (m, 1H), 3.86 (s, 3H), 4.10–4.12 (m, 1H), 6.97–7.00 (m, 2H), 7.21–7.33 (m, 7H), 7.34–7.43 (m, 5H).

6.1.18. *L*-Phenylalanyl-*N*¹-[(2*R*)-2-amino-3-phenylpropyl]-*L*-cysteinamide hydrochloride (B1)

Yield: 67%, mp = 170–172 °C. ESI-MS *m/z*: 401.5 (M+H)⁺; ¹H NMR (D₂O) δ 2.64–2.71 (*J*₁ = 3.9, *J*₂ = 14.4, dd, 1H), 2.80–2.85 (m, 2H), 2.86–2.93 (*J*₁ = 4.2, *J*₂ = 13.8, dd, 1H), 3.04–3.05 (*J* = 3.6, d, 2H), 3.22–3.27 (*J*₁ = 3.9, *J*₂ = 13.5, dd, 1H), 3.28–3.34 (*J*₁ = 4.5, *J*₂ = 13.8, dd, 1H), 3.48–3.53 (m, 1H), 4.12–4.15 (*J* = 7.2, t, 1H), 4.46–4.48 (*J* = 7.2, t, 1H), 7.06–7.15 (m, 5H), 7.17–7.26 (m, 5H).

6.1.19. Glycyl-*N*¹-[(2*R*)-2-amino-3-phenylpropyl]-*L*-cysteinamide hydrochloride (B2)

Yield: 80%, mp = 164–166 °C. ESI-MS *m/z*: 311.2 (M+H)⁺; ¹H NMR (D₂O) δ 2.92–2.99 (m, 2H), 3.07–3.14 (m, 2H), 3.21–3.22 (*J* = 3.3, d, 2H), 3.79 (s, 2H), 4.01–4.06 (m, 1H), 4.54–4.57 (*J* = 6.9, t, 1H), 7.28–7.39 (m, 5H).

6.1.20. *L*-Cysteinyl-*N*¹-[(2*R*)-2-amino-3-phenylpropyl]-*L*-cysteinamide hydrochloride (B3)

Yield: 72%, mp = 197–200 °C. ESI-MS *m/z*: 357.6 (M+H)⁺; ¹H NMR (D₂O) δ 2.73–2.79 (m, 2H), 2.85–2.93 (m, 4H), 3.36–3.43 (m, 2H), 3.82–3.87 (m, 1H), 4.07–4.11 (*J* = 5.7, t, 1H), 4.33–4.36 (*J* = 6.3, t, 1H), 7.25–7.35 (m, 5H).

6.1.21. *L*-Leucyl-*N*¹-[(2*R*)-2-amino-3-phenylpropyl]-*L*-cysteinamide hydrochloride (B4)

Yield: 62%, mp = 146–148 °C. ESI-MS *m/z*: 367.5 (M+H)⁺; ¹H NMR (D₂O) δ 1.02–1.05 (m, 6H), 1.33–1.37 (m, 1H), 1.71–1.73 (m, 2H), 2.84–2.91 (m, 2H), 3.02–3.04 (*J* = 6.9, d, 2H), 3.46–3.55 (m, 2H), 3.67–3.70 (m, 1H), 3.74–3.77 (m, 1H), 3.96–4.01 (*J* = 14.4, t, 1H), 7.25–7.42 (m, 5H).

6.1.22. *L*-Methionyl-*N*¹-[(2*R*)-2-amino-3-phenylpropyl]-*L*-cysteinamide hydrochloride (B5)

Yield: 61%, mp = 137–140 °C. ESI-MS *m/z*: 385.0 (M+H)⁺; ¹H NMR (D₂O) δ 1.51–1.56 (m, 2H), 2.13–2.16 (m, 2H), 2.19 (s, 3H), 2.62–2.70 (m, 2H), 2.94–3.02 (m, 2H), 3.37–3.41 (m, 1H), 3.42–3.47 (m, 2H), 4.11–4.15 (m, 1H), 4.65–4.68 (m, 1H), 7.31–7.41 (m, 5H).

6.1.23. *L*-Lysyl-*N*¹-[(2*R*)-2-amino-3-phenylpropyl]-*L*-cysteinamide hydrochloride (B6)

Yield: 59%, mp = 80–82 °C. ESI-MS *m/z*: 382.5 (M+H)⁺; ¹H NMR (D₂O) δ 1.51–1.56 (m, 2H), 1.72–1.77 (m, 2H), 1.91–1.95 (m, 2H), 2.68–2.75 (m, 2H), 2.83–2.89 (m, 2H), 2.98–3.03 (*J* = 15, t, 2H),

3.68–3.74 (m, 2H), 3.82–3.87 (m, 1H), 4.02–4.05 (m, 1H), 4.32–4.37 (J = 14.1, t, 1H), 7.32–7.41 (m, 5H).

6.1.24. L-Ornithyl-*N*¹-[(2*R*)-2-amino-3-phenylpropyl]-L-cysteinamide hydrochloride (B7)

Yield: 55%, mp = 161–164 °C. ESI-MS *m/z*: 368.4 (M+H)⁺; ¹H NMR (D₂O) δ 1.61–1.66 (m, 2H), 1.83–1.89 (m, 2H), 2.54–2.59 (m, 2H), 2.78–2.82 (m, 2H), 3.06–3.11 (J = 14.7, t, 2H), 3.56–3.61 (m, 2H), 3.74–3.81 (m, 1H), 4.09–4.15 (m, 1H), 4.28–4.33 (J = 14.4, t, 1H), 7.22–7.37 (m, 5H).

6.1.25. L-Isoleucyl-*N*¹-[(2*R*)-2-amino-3-phenylpropyl]-L-cysteinamide hydrochloride (B8)

Yield: 63%, mp = 228–230 °C. ESI-MS *m/z*: 367.2 (M+H)⁺; ¹H NMR (MeOD) δ 0.93–0.96 (J = 6.6, d, 3H), 1.06–1.10 (J = 14.1, t, 3H), 1.27–1.31 (m, 2H), 1.58–1.62 (m, 1H), 2.86–2.93 (m, 2H), 3.00–3.09 (m, 1H), 3.21–3.28 (J₁ = 4.2, J₂ = 14.1, dd, 1H), 3.36–3.43 (J₁ = 5.1, J₂ = 14.4, dd, 1H), 3.51–3.59 (J₁ = 5.7, J₂ = 14.7, dd, 1H), 3.68–3.72 (m, 1H), 3.89–3.95 (m, 1H), 4.63–4.68 (J = 14.7, t, 1H), 7.30–7.39 (m, 5H).

6.1.26. L-Alanyl-*N*¹-[(2*R*)-2-amino-3-phenylpropyl]-L-cysteinamide hydrochloride (B9)

Yield: 64%, mp = 170–173 °C. ESI-MS *m/z*: 353.3 (M+H)⁺; ¹H NMR (D₂O) δ 0.77–0.78 (J = 3, d, 3H), 0.92–0.94 (J = 4.5, d, 3H), 1.88–1.97 (m, 1H), 2.78–2.85 (m, 2H), 2.86–2.93 (m, 2H), 3.26–3.33 (m, 2H), 3.34–3.40 (m, 1H), 3.58–3.61 (m, 1H), 3.70–3.76 (m, 1H), 7.18–7.31 (m, 5H).

6.1.27. *N*¹-[(2*R*)-2-Amino-3-phenylpropyl]-*N*-(6-aminohexanoyl)-L-cysteinamide hydrochloride (B10)

Yield: 72%, mp = 172–178 °C. ESI-MS *m/z*: 367.5 (M+H)⁺; ¹H NMR (MeOD) δ 0.94–1.00 (m, 2H), 1.43–1.48 (m, 2H), 1.63–1.69 (m, 2H), 2.01–2.04 (J = 7.2, t, 2H), 2.32–2.35 (J = 9.6, t, 2H), 2.92–2.95 (m, 2H), 2.96–2.98 (m, 2H), 3.21–3.26 (m, 2H), 3.31–3.34 (m, 1H), 4.39–4.43 (J = 12.3, t, 1H), 7.29–7.41 (m, 5H).

6.1.28. *N*¹-[(2*R*)-2-Amino-3-phenylpropyl]-*N*-(2,4-dichlorobenzoyl)-L-cysteinamide hydrochloride (B11)

Yield: 70%, mp = 145–148 °C. ESI-MS *m/z*: 427.3 (M+H)⁺; ¹H NMR (D₂O) δ 2.57–2.64 (m, 2H), 2.78–2.86 (m, 1H), 2.91–2.98 (m, 1H), 3.26–3.32 (J₁ = 6.6, J₂ = 14.4, dd, 1H), 3.40–3.46 (J₁ = 4.5, J₂ = 14.7, dd, 1H), 3.53–3.62 (m, 1H), 4.01–4.06 (J = 14.7, t, 1H), 7.21–7.33 (m, 8H).

6.1.29. L-Isoleucyl-*N*¹-[(2*R*)-2-amino-3-phenylpropyl]-L-leucinamide hydrochloride (C1)

Yield: 73%, mp = 153–155 °C. ESI-MS *m/z*: 377.8 (M+H)⁺; ¹H NMR (D₂O) δ 0.72–0.73 (J = 4.5, t, 3H), 0.76–0.78 (J = 6.3, d, 6H), 0.84–0.86 (J = 6, d, 3H), 1.03–1.08 (m, 1H), 1.31–1.37 (m, 2H), 1.48–1.54 (m, 2H), 1.80–1.83 (m, 1H), 2.69–2.76 (J₁ = 4.2, J₂ = 13.5, dd, 1H), 2.87–2.92 (J₁ = 4.8, J₂ = 14.2, dd, 1H), 3.27–3.33 (J₁ = 4.8, J₂ = 13.5, dd, 1H), 3.38–3.44 (J₁ = 4.5, J₂ = 13.5, dd, 1H), 3.55–3.59 (m, 1H), 3.73–3.77 (m, 1H), 4.16–4.20 (J = 12, t, 1H), 7.15–7.28 (m, 5H).

6.1.30. L-Leucyl-*N*¹-[(2*R*)-2-amino-3-phenylpropyl]-L-leucinamide hydrochloride (C2)

Yield: 79%, mp = 108–112 °C. ESI-MS *m/z*: 377.5 (M+H)⁺; ¹H NMR (D₂O) δ 0.74–0.76 (J = 6.0, d, 6H), 0.81–0.84 (J = 5.7, d, 6H), 0.92–0.97 (m, 1H), 1.38–1.44 (m, 2H), 1.57–1.62 (m, 2H), 1.82–1.84 (m, 1H), 3.11–3.17 (J₁ = 5.4, J₂ = 13.8, dd, 1H), 3.19–3.26 (J₁ = 5.7, J₂ = 14.4, dd, 1H), 3.40–3.47 (J₁ = 6, J₂ = 14.4, dd, 1H), 3.52–3.58 (J₁ = 6.3, J₂ = 13.2, dd, 1H), 3.62–3.67 (m, 1H), 3.77–3.83 (m, 1H), 4.56–4.60 (J = 8.7, t, 1H), 7.20–7.36 (m, 5H).

6.1.31. L-Alanyl-*N*¹-[(2*R*)-2-amino-3-phenylpropyl]-L-leucinamide hydrochloride (C3)

Yield: 73%, mp = 164–166 °C. ESI-MS *m/z*: 335.8 (M+H)⁺; ¹H NMR (D₂O) δ 0.79–0.82 (J = 6.3, d, 3H), 0.84–0.86 (m, 4H), 1.38–1.44 (m, 3H), 1.60–1.64 (m, 2H), 2.81–2.88 (J₁ = 6.3, J₂ = 13.8, dd, 1H), 2.94–3.01 (J₁ = 6.6, J₂ = 14.1, dd, 1H), 3.32–3.38 (J₁ = 4.2, J₂ = 13.5, dd, 1H), 3.43–3.49 (J₁ = 4.2, J₂ = 12.3, dd, 1H), 3.61–3.67 (m, 1H), 4.01–4.08 (m, 1H), 4.24–4.27 (J = 9, t, 1H), 7.23–7.37 (m, 5H).

6.1.32. Glycyl-*N*¹-[(2*R*)-2-amino-3-phenylpropyl]-L-leucinamide hydrochloride (C4)

Yield: 71%, mp = 117–119 °C. ESI-MS *m/z*: 321.5 (M+H)⁺; ¹H NMR (D₂O) δ 0.83–0.85 (J = 6.6, d, 6H), 1.21–1.26 (m, 1H), 1.61–1.66 (m, 2H), 2.91–3.01 (m, 2H), 3.31–3.38 (m, 2H), 3.63–3.69 (m, 1H), 3.90 (s, 2H), 4.36–4.39 (J = 8.7, t, 1H), 7.28–7.41 (m, 5H).

6.1.33. L-Methionyl-*N*¹-[(2*R*)-2-amino-3-phenylpropyl]-L-leucinamide hydrochloride (C5)

Yield: 67%, mp = 126–129 °C. ESI-MS *m/z*: 395.4 (M+H)⁺; ¹H NMR (MeOD) δ 0.90–1.02 (m, 6H), 1.38–1.51 (m, 1H), 1.68–1.79 (m, 2H), 2.12 (s, 3H), 2.13–2.16 (m, 2H), 2.56–2.69 (m, 2H), 3.15–3.22 (J₁ = 6.6, J₂ = 13.2, dd, 1H), 3.24–3.31 (m, 1H), 3.40–3.41 (m, 1H), 3.45–3.47 (m, 1H), 3.96–4.00 (m, 1H), 4.06–4.15 (m, 1H), 4.53–4.56 (J = 9, t, 1H), 7.23–7.38 (m, 5H).

6.1.34. L-Tyrosyl-*N*¹-[(2*R*)-2-amino-3-phenylpropyl]-L-leucinamide hydrochloride (C6)

Yield: 70%, mp = 158–160 °C. ESI-MS *m/z*: 427.4 (M+H)⁺; ¹H NMR (MeOD) δ 0.94–1.00 (m, 6H), 1.40–1.45 (m, 1H), 1.72–1.76 (m, 1H), 2.85–2.93 (m, 2H), 2.97–3.07 (m, 2H), 3.14–3.22 (m, 2H), 4.02–4.05 (m, 1H), 4.08–4.15 (m, 1H), 4.55–4.60 (J = 15.3, t, 1H), 6.78–6.81 (m, 2H), 7.13–7.15 (m, 2H), 7.25–7.35 (m, 5H).

6.1.35. *N*¹-[(2*R*)-2-Amino-3-phenylpropyl]-*N*-(6-aminohexanoyl)-L-leucinamide hydrochloride (C7)

Yield: 63%, mp = 101–105 °C. ESI-MS *m/z*: 377.7 (M+H)⁺; ¹H NMR (MeOD) δ 0.90–0.96 (m, 6H), 0.97–1.04 (m, 2H), 1.12–1.16 (m, 1H), 1.33–1.40 (m, 2H), 1.42–1.50 (m, 2H), 1.60–1.66 (m, 2H), 2.16–2.22 (J = 10.5, t, 2H), 2.97–3.04 (m, 2H), 3.07–3.12 (J = 14.7, t, 2H), 3.27–3.31 (m, 2H), 3.71–3.77 (m, 1H), 4.47–4.52 (J = 15, t, 1H), 7.27–7.41 (m, 5H).

6.2. Biological materials and methods

6.2.1. In vitro APN assay

IC₅₀ values against APN were determined as previously described and using L-Leu-*p*-nitroanilide as substrate and Microsomal aminopeptidase from Porcine Kidney Microsomes (Sigma) as the enzyme in 50 mM PBS, pH 7.2, at 37 °C. The hydrolysis of the substrate was monitored by following the change in the absorbance measured at 405 nm with the UV-vis spectrophotometer Pharmacia LKB, Biochrom 4060. All solutions of inhibitors were prepared in the assay buffer, and pH was adjusted to 7.5 by the addition of 0.1 M HCl or 0.1 M NaOH. All inhibitors were preincubated with APN for 30 min at room temperature. The assay mixture, which contained the inhibitor solution (concentration dependent on the inhibitor), the enzyme solution (4 μg/mL final concentration), and the assay buffer, was adjusted to 200 μL.

6.2.2. MTT assay

HL-60 Cell was grown in RPMI1640 medium containing 10% FBS at 37 °C in 5% CO₂ humidified incubator. Cell proliferation was determined by the MTT (3-[4,5-dimethyl-2-thiazolyl]-2,5-diphenyl-2*H*-tetrazolium bromide) assay. Briefly, cells were plated in a 96-well plate at 10,000 cells per well, cultured for 4 h in complete growth medium, then treated with 1600, 800, 400, 200, 100 μg/mL

of compounds for 48 h. 0.5% MTT solution was added to each well. After further incubation for 4h, formazan formed from MTT was extracted by adding DMSO and mixing for 15 min. Optical density was read with an ELISA reader at 570 nm.

Acknowledgments

This work was supported by National Nature Science Foundation of China (Grant Nos. 30772654, 90713041) and the Ph.D. Programs Foundation of Ministry of Education of P.R. China (No. 20060422029) and National High Technology Research and Development Program of China (863 Project; Grant No. 2007AA02Z314).

References and notes

- Dixon, J.; Kaklamanis, L.; Turley, H.; Hickson, I. D.; Leek, R. D.; Harris, A. L.; Gatter, K. C. *J. Clin. Pathol.* **1994**, 47, 43.
- Look, A. T.; Ashmun, R. A.; Shapiro, L. H.; Stephen, S. C.; Peiper, C. J. *Clin. Invest.* **1989**, 83, 1299.
- Shimizu, T.; Tani, K.; Hase, K.; Ogawa, H.; Huang, L.; Shinomiya, F.; Sone, S. *Arthritis Rheum.* **2002**, 46, 2330.
- Sato, Y. *Biol. Pharm. Bull.* **2004**, 772, 776.
- Bedir, A.; Ozener, I. C.; Emerk, K. *Nephron* **1996**, 74, 110.
- Sloane, P. D.; Zimmerman, S.; Suchindran, C.; Reed, P.; Wang, L.; Boustani, M.; Sudha, S. *Annu. Rev. Public Health* **2002**, 23, 213.
- Xu, W. F.; Li, Q. B. *Curr. Med. Chem. Anti-Cancer Agents* **2005**, 53, 281.
- Babine, R. E.; Bender, S. L. *Chem. Rev.* **1997**, 97, 1359.
- Leung, D.; Abbenante, G.; Fairlie, D. P. *J. Med. Chem.* **2000**, 43, 305.
- Umezawa, H.; Aoyagi, T.; Suda, H.; Hamada, M.; Takeuchi, T. *J. Antibiot. (Tokyo)* **1976**, 29, 97.
- Onohara, Y.; Nakajima, Y.; Ito, K., et al *Acta Crystallogr.* **2006**, 62, 699.
- Kiyoshi, I.; Yoshitaka, N.; Tadashi, Y., et al *J. Biol. Chem.* **2006**, 281, 33664.
- Addlagatta, A.; Gay, L.; Matthews, B. W. *Proc. Natl. Acad. Sci. U.S.A.* **2006**, 103, 13339.
- Li, Q. B.; Fang, H.; Xu, W. F. *Bioorg. Med. Chem. Lett.* **2007**, 17, 2935.
- Wang, Q.; Chen, M. Y.; Zhu, H. W.; Zhang, J.; Fang, H.; Wang, B. H.; Xu, W. F. *Bioorg. Med. Chem.* **2008**, 16, 5473.
- Wang, J. L.; Xu, W. F. *J. Chem. Res. Synop.* **2003**, 12, 789.
- Shang, L. Q.; Maeda, T.; Xu, W. F.; Kishioka, S. *J. Enzyme Inhib. Med. Chem.* **2008**, 23, 198.
- Zhu, H. W.; Fang, H.; Wang, L.; Hu, W.; Xu, W. F. *Drug Discovery Ther.* **2008**, 2, 52.
- Shang, L. Q.; Wang, Q.; Fang, H.; Mu, J. J.; Wang, X. J.; Yuan, Y. M.; Wang, B. H.; Xu, W. F. *Bioorg. Med. Chem.* **2008**, 16, 9984.
- Beaulieu, P. L.; Wernic, D., et al *Tetrahedron Lett.* **1995**, 36, 3317.
- Fournié-Zaluski, M.; Coric, P.; Turcaud, S.; Bruetschy, L.; Lucas, E.; Noble, F.; Roques, B. P. *J. Med. Chem.* **1992**, 35, 1259.